Scientific paper

Ab initio and Density Functional Theory Studies on Nitrosoketene Tautomers

Lemi Türker* and Taner Atalar

Middle East Technical University, Department of Chemistry, 06531Ankara, Turkey

** Corresponding author: E-mail: lturker@metu.edu.tr, Fax: 90-312-2103200*

Received: 27-06-2007

Abstract

The structural stabilities of nitrosoketene and its tautomers were investigated using *ab initio* and DFT method of calculations employing 6-31++G(d,p), cc-pVDZ basis sets. Additionally MP2/6-31++G(d,p) and G3 calculations were performed. Nitrosoketene (I) and structure III were found to be the most stable and the least stable tautomers, respectively. The gas phase deprotonation energies have been determined using Gaussian-2 (G2) method. According to the deprotonation calculations, all the species should be more acidic than water and the acidity order is III > II > I.

***Keywords*:** Nitrosoketene, tautomers, deprotonation energy, *ab initio*, DFT treatment.

1. Introduction

The synthetic utility of ketenes in organic chemistry has attracted the attention of both the synthetic and theoretical chemists. For example, thermal decomposition of ketenes is considered as a suitable source of carbenes and their catalyzed pyrolysis provides polymerization of ketenes[1]. Because of the interesting electronic structure of ketenes, these species have frequently been the subject of investigation by molecular orbital (MO) methods.[2–7] These studies have focused mostly on the electronic structure of ketene itself, [8] the reaction of ketenes with protons[9] and nucleophiles,[10] cycloaddition of ketenes with alkenes[11] and dialkoxyalkynes[12] and rearrangement of conjugated ketenes.[13]

Many substituted ketenes have been generated and their properties observed[14]. One of the important substituted ketenes is nitrosoketene (I) (see Figure 1). The pyrolysis of isonitroso Meldrum's acid generates nitrosoketene (I) in the temperature-controlled sample cell under vacuum and temperatures above 80 °C.[15]

In the literature there are some studies concerning nitrosoketene.[16,17] Birney and co-workers[18] studied the cycloaddition of nitrosoketene (I) with formaldehyde, acetone and 2-propenal using *ab initio* molecular orbital theory (MP2/6-31G (d)). Matsui and co-workers investigated the conformations of the nitrosoketene, (they call them *E*- and *Z*-isomers, generated via the pyrolysis of isonitroso Meldrum's acid) by their characteristic vibrational wavenumbers[19]. Matsui and co-workers also worked on FTIR and *ab initio* studies of gaseous nitrosoketene (I) and they experimentally found that at temperatures exceeding 160 °C, nitrosoketene (I) undergoes decarbonylation. On the other hand, Badawi and co-workers investigated the structural stability and vibrational spectra of nitroso and nitroketenes.[20] However, there is nothing mentioned

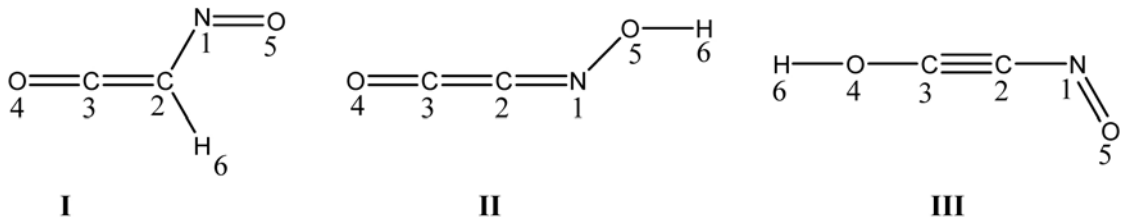

Figure 1. The chemical structures of nitrosoketene (I) and its tautomers (II and III), and numbering of the atoms.

about the tautomeric forms of it (to the best of our knowledge). Furthermore, there is no reported estimate of the deprotonation energy for them in the literature. In the present study, nitrosoketene (I) and its some tautomers (II and III) have been subjected to *ab initio* and DFT type calculations. Moreover, in order to understand stability of the species better, the deprotonation energies of them have been accurately calculated.

2. Method

The initial geometry optimizations for all the structures leading to energy minima were achieved first by using MM2 method followed by semi-empirical PM3[21,22] at the restricted level[23,24]. Then, geometry optimizations were carried out within the framework of density functional theory (DFT, B3LYP)[25–29] at the level of 6-31++G(d,p) and cc-pVDZ (restricted closed-shell). In addition to DFT calculations, *ab initio* RHF/6-31++G(d,p) and RHF/cc-pVDZ calculations[30] were performed. Furthermore, single point MP2 calculations were carried out (for *ab initio* calculations) in order to obtain more accurate energy data. For each case (DFT and *ab initio* calculations, using the same basis sets employed in the corresponding geometry optimizations) the vibrational analyses were done. The total electronic energies are corrected for zero-point energy. The normal mode analysis for each structure yielded no imaginary frequency. This indicates that the geometry optimized structure of each molecule corresponds to at least a local minimum on the potential energy surface.

Also initially optimized molecules at the Hartree-Fock (HF) level were subjected to Gaussian-2 (G2),[31] Gaussian-3 (G3)[32] and complete basis set method CBS-Q[33–38] calculations to obtain very accurate energies. Additionally, deprotonation energies were calculated by using G2 method which is mentioned as a very good method for calculation of this property in the literature.[39] Pople and co-workers[31,32] have developed the Gaussian methods (G1, G2, G3, and MP2 variants), which are extrapolation schemes similar to the CBS model chemistries. The G2, G3, and CBS-Q model chemistries are state-of-the-art models for accurate thermochemistry.[40–42] All these computations were performed by using Gaussian 03 package program[43].

3. Results and Discussion

Because of the interesting electronic structure and reactivity of nitrosoketene (I), we investigated its structure and tautomeric forms (structures II and III). From the present calculations, the molecules were predicted to exist in the planar conformations. Figure 2 shows the geometry optimized structures of the present concern (B3LYP/cc-pVDZ). Note that, of the various calculations

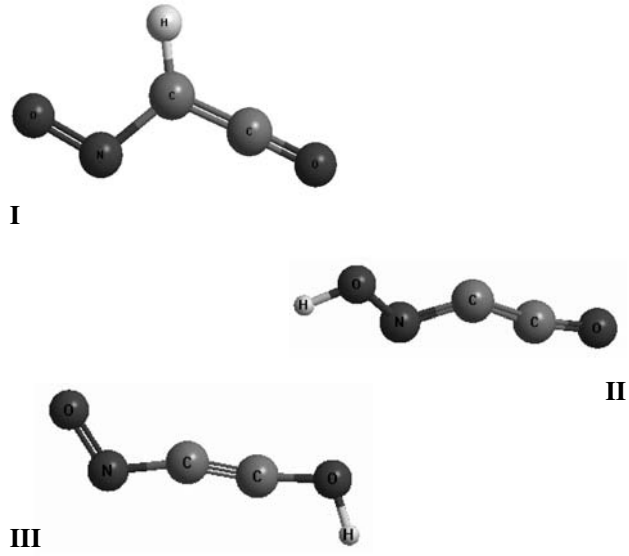

Figure 2. The geometry optimized (B3LYP/cc-pVDZ) structures of present concern.

performed, only the B3LYP/cc-pVDZ geometry optimized structures have been shown in Figure 2 for the sake of clarity. InTable 1, the presently calculated geometric parameters of nitrosoketene (I) at various theoretical levels are presented. The B3LYP method predicts longer bond length of C2-N1 than the *ab initio* method does (see Table 1). The geometry optimized structures have C_s type molecular point group for nitrosoketene (I). The results of the calculations reveal that nitrosoketene (I) exists in the E-conformation (staggered conformation, see Figure 2) rather than the Z-conformation (eclipsed conformation, conformations according to C2-N1 sigma bond), this result is consistent with the earlier literature data.[19,20] Badawi and co-workers[20] studied nitrosoketene (I) and nitroketene and according to their calculations, the rotational barrier of the NO group in nitrosoketene (I) was calculated to be about 18 kcal/mol. Tables 2 and 3 show some geometrical features of the tautomers. As seen in the tables, the level of calculations do not yield very different bond lengths. The geometry optimized structures of tautomers II and III are somewhat interesting. In the case of the structure II, N1-C2-C3 bond angle (see Figure 1 for numbering of the atoms) is found to be different than 180° (e.g. 122.5° at RHF/cc-pVDZ, see Table 2), C2-C3-O4 and N1-C2-C3 bond angles are also found to be 164.2° and 131.5°, respectively at B3LYP/ cc-pVDZ. The C–H bond length is calculated to be longer than the O–H bond length (as expected) and the O–H bond length in tautomer III is found to be somewhat longer than the one in tautomer II. It can be seen from Tables 1–3 that the result of DFT calculations yield longer bond lengths as compared to HF calculations whereas, the presently used calculation methods show a parallelism in reflecting the

Table 1. Calculated structural parameters (Å and degrees) and total dipole moment (in Debye, 1 Debye = $3.336*10^{-30}$ C. m) of nitrosoketene (**I**).

	RHF[a]	RHF[b]	B3LYP[a]	B3LYP[b]
Bond length				
$r(N_1–C_2)$	1.401	1.395	1.433	1.419
$r(C_2=C_3)$	1.332	1.332	1.338	1.339
$r(C_3=O_4)$	1.129	1.130	1.159	1.158
$r(N_1=O_5)$	1.180	1.186	1.216	1.224
$r(C_2–H_6)$	1.080	1.072	1.093	1.086
Bond angle				
$(N_1C_2C_3)$	115.9	115.5	118.1	117.0
$(C_2C_3O_4)$	179.1	179.0	178.6	178.8
$(C_2N_1O_5)$	114.5	114.8	113.0	113.6
$(C_3C_2H_6)$	120.5	115.5	120.2	120.9
$(C_3C_2N_1O_5)$	180.0	180.0	180.0	180.0
Dipole moment	2.75	2.91	2.60	3.02

a: cc–pVDZ, b: 6–31++G(d,p)

Table 2. Calculated structural parameters (Å and degrees) and total dipole moment (in Debye, 1 Debye = $3.336*10^{-30}$ C. m) of tautomer (**II**).

	RHF[a]	RHF[b]	B3LYP[a]	B3LYP[b]
Bond length				
$r(N_1=C_2)$	1.265	1.261	1.285	1.281
$r(C_2=C_3)$	1.361	1.361	1.329	1.328
$r(C_3=O_4)$	1.127	1.128	1.169	1.169
$r(N_1-O_5)$	1.339	1.342	1.377	1.382
$r(O_5–H_6)$	0.946	0.945	0.973	0.971
Bond angle				
$(N_1C_2C_3)$	122.5	121.4	131.5	130.4
$(C_2C_3O_4)$	163.7	164.1	164.2	164.3
$(C_2N_1O_5)$	111.9	112.3	111.1	111.5
$(C_3C_2N_1O_5)$	179.9	180.0	179.9	180.0
Dipole moment	1.86	1.99	2.12	2.14

Table 3. Calculated structural parameters (Å and degrees) and total dipole moment (in Debye, 1 Debye = $3.336*10^{-30}$ C. m) of tautomer (**III**).

	RHF[a]	RHF[b]	B3LYP[a]	B3LYP[b]
Bond length				
$r(N_1–C_2)$	1.388	1.382	1.372	1.362
$r(C_2=C_3)$	1.191	1.187	1.225	1.219
$r(C_3–O_4)$	1.292	1.291	1.299	1.298
$r(N_1=O_5)$	1.176	1.183	1.223	1.232
$r(O4–H_6)$	0.952	0.949	0.976	0.972
Bond angle				
$(N_1C_2C_3)$	173.2	173.7	163.4	168.6
$(C_2C_3O_4)$	179.6	178.8	171.5	177.6
$(C_2N_1O_5)$	115.5	115.5	117.9	117.4
$(C_3C_2N_1O_5)$	179.9	179.9	180.0	180.0
$(H_6O_4C_3C_2)$	179.4	179.9	180.0	180.0
Dipole moment	3.71	3.81	4.71	4.87

a: cc–pVDZ , b: 6–31++G(d,p)

geometrical differences existing among the concerned species. Considering the computed total dipole moment values at DFT and HF methods, the most polar tautomer occurs to be tautomer III and the order of the total dipole moment is in the order of III > I > II (see the Tables 1,2 and 3). It is clear from Figure 3 that why the tautomer III has higher dipole moment than the other species. In the case of the tautomer II, bond dipoles oriented in the molecule so that the net dipole moment is the smallest one among them, the most uniform electrostatic potential map belongs to it.

Figure 3 shows the 3D-molecular electrostatic potential $V_s(r)$ maps for the species (isopotential value of 1.000 eV) calculated at B3LYP/cc-pVDZ level. The species considered generate an electrostatic potential around them due to the overall effect of positive and negative charge distribution. In Figure 3, the darker and lighter regions are negative and positive electrostatic potentials, respectively. As evident from the figure, the lighter regions (positive fields) are predominating in the structures. A characteristic feature of the $V_s(r)$ of the nitroaromatics, nitroheterocycles, and nitroalkanes is a buildup of positive potential, with a local $V_{s,max}$ above the C–NO_2 bonds[44–46]. This has not been observed to be associated with chemical bonds in general[44–46]. It was shown that this positive build up provides a channel for the initial approach of a nucleophile [47,48]. More relevant is the fact that $V_{s,max}$, correlates reasonably well with the strength of the bond, provided that the size of the molecule is taken into account [45,46], so that for molecules with approximately the same surface area, the more positive is the $V_{s,max}$ above the bond, the weaker the bond is. In Figure 3, it is seen, that some regions of negative V_r are associated with lone pairs and due to the π electrons of the unsaturated systems. In the great majority of organic molecules (like presently considered species), the regions of the negative $V_s(r)$ are smaller in area but often quite strong (see Figure 3), while the more extensive positive regions are significantly weaker. In energetic molecules, on the other hand, the positive $V_s(r)$ still covers the larger areas but now tends to be much stronger than the negative[49]. The molecular electrostatic potential offers a means of characterizing molecules at a fundamental level. Furthermore, Table 4 shows the computed Mulliken atomic charges of nitrosoketene (I) and its tautomers II and III. The residual charges on N1 atom in tautomer II has higher than the charges of N1 atom in the other species, and the most positively charged hydrogen atom is found in tautomer III.

Table 5 shows calculated energies of the tautomers (relative to most stable tautomer I) at different levels of theory (the total electronic energies are corrected for ZPVE). All the results in the table show that the stability order is I > II > III. Among the calculation methods performed, the lowest energies are obtained at B3LYP/cc-pVDZ level of theory. As for the tautomeric form II, the to-

Table 4. Computed Mulliken atomic charges of nitrosoketene (**I**) and its tautomers (**II** and **III**).

			B3LYP/cc-pVDZ			
	N1	C2	C3	O4	O5	H6
I	0.004	–0.008	0.176	–0.031	–0.194	0.053
II	–0.061	–0.103	0.176	–0.070	–0.105	0.163
III	–0.002	0.035	0.054	–0.097	–0.182	0.192
			CBS–Q			
	N1	C2	C3	O4	O5	H6
I	–0.070	–0.059	0.455	–0.310	–0.144	0.128
II	–0.199	–0.049	0.300	–0.265	–0.089	0.303
III	–0.065	0.132	0.206	–0.444	–0.142	0.313
			G3			
	N1	C2	C3	O4	O5	H6
I	–0.068	–0.051	0.455	–0.320	–0.151	0.135
II	–0.210	0.245	0.069	–0.266	–0.136	0.299
III	–0.096	0.119	0.268	–0.460	–0.151	0.320

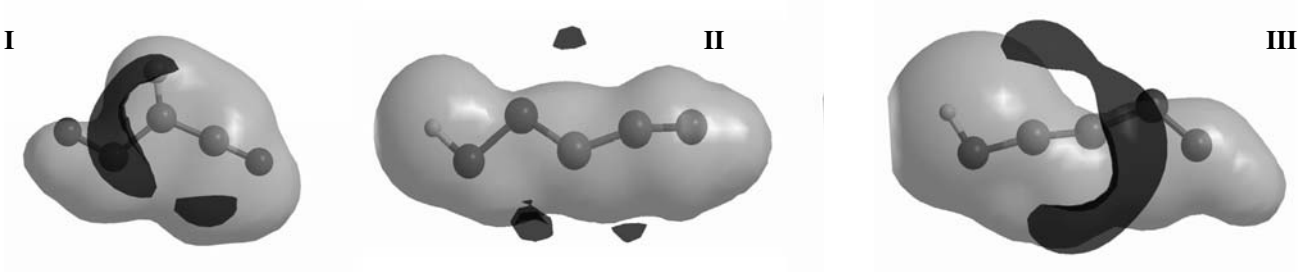

Figure 3. Molecular electrostatic potential maps of the species concerned (B3LYP/cc-pVDZ).

tal energy is more favorable than the tautomeric form III (in all the levels of theory). The calculated energy difference between the most favorable and unfavorable species is 185 (B3LYP/cc-pVDZ), 175 (G3) and 166 kJ/mol (CBS-Q) in the gas phase (see Table 5). Note that the proton shifts among these tautomers are accompanied by some sort of hybridization change or bond type.

Also, deprotonation energies of the species concerned have been calculated. In order to calculate the deprotonation energies, G2 calculations have been performed, because in the literature it is mentioned as the reliable method for the calculation of this property [38]. The free energies for the gas phase deprotonation of nitrosoketene(I) and its tautomers II and III are calculated according to the reactions shown in scheme 1. The value for G_{gas} (H^+) = –26.28 kJ/mol, comes from the Sackur-Tetrode equation.[50,51] The calculation of free energies in the gas phase uses a reference state of 1 atm and 298.15 K. The computed free energies for the deprotonation of nitrosoketene (I) and tautomers II and III are 1403.73, 1358.55 and 1224.24 kJ/mol, respectively. As expected, the triple bond in tautomer III enhances the acidity of hydrogens. These results have been supported by the residual charges on hydrogen atoms derived from the Mulliken population analysis using different theoretical approaches (see Table 4). However, a question can be asked that is how the deprotonation energy of concerned species is compared to that of water. We have calculated the deprotonation energy

Table 5. Computed relative energies, ΔE, (relative to tautomer **I**, in kJ/mol) of the species concerned.

	RHF[a]	**RHF[b]**	**B3LYP[a]**	**B3LYP[b]**	**G3**	**CBS–Q**
II	89	84	50	48	58	46
	(55)	(51)				
III	190	185	185	184	175	166
	(192)	(190)				

a: cc–pVDZ b: 6–31++G(d,p). The values in the parentheses indicate that single-point MP2 calculation after RHF geometry optimizations.

value of water to be 1602.89 kJ/mol at the same level of theory (G2). In the literature, gas phase deprotonation energy value of water was calculated as 1626.32 kJ/mol at CCSD(T)/aug-cc-pVQZ level of theory.[52] Comparison of the computed energies suggests that nitrosoketene (I) and its tautomers (II and III) should release proton more readily compared to water in the gas phase.

Figure 5 shows the frontier molecular orbitals of the presently considered molecules. The chemical reactivity is affected by the interaction between the HOMO of the nucleophile and LUMO of the electrophile. By studying the HOMO and LUMO characteristics, it is foreseen whether or not the reaction is feasible. The frontier molecular orbital energy gap of the tautomers obtained at various theoretical levels. As seen there, in most of the cases, LUMOs mainly possess π-type symmetry. In the cases of tautomers II and III, there exists an extended conjugation involving the hydroxy group. Table 6 tabulates the HOMO and LUMO energies of the structures considered at different levels of theory. As the energy difference between HOMO-LUMO energy levels ($\Delta\varepsilon = \varepsilon_{LUMO} - \varepsilon_{HOMO}$) is considered, the order is I > III > II at all the levels (except DFT and MP2 results). Whereas the order obtained at DFT (B3LYP) is I > II > III and for MP2 the order is III > I > II. As for the comparison of the calculation methods, the computed LUMO energies in the case of DFT were found to be low (more negative value), on the contrary the HOMO energies were obtained as quite high (less negative value) compared to other methods. Generally, the greater value of energy gap resulting from higher energy of LUMO and lower energy of HOMO indicates that neither losing nor capturing of electron would happen on the compound easily, so it is more stable.

Table 7 tabulates various calculated geometrical and physicochemical properties of the molecules (based on the MP2/cc-pVDZ and MP2/6-31++G(d,p) single point calculations after RHF geometry optimizations by using the corresponding basis sets). Note that some data in the table are obtained based on the group additivities and independent of the geometry optimizations (such as refractivities and polarizabilities).

Area, volume, refractivity and polarizability values are in the order of 10^{-20} m^2, 10^{-30} m^3, 10^{-30} m^3, 10^{-30} m^3, respectively.

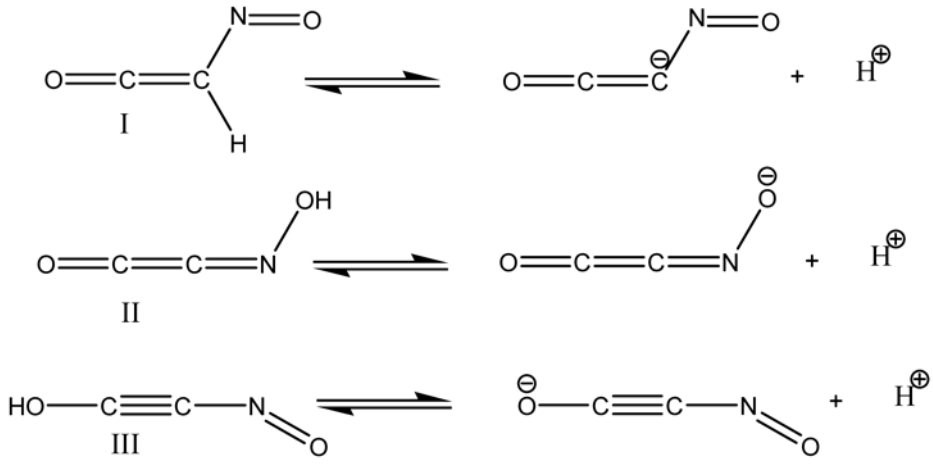

Scheme 1. Deprotonation reactions.

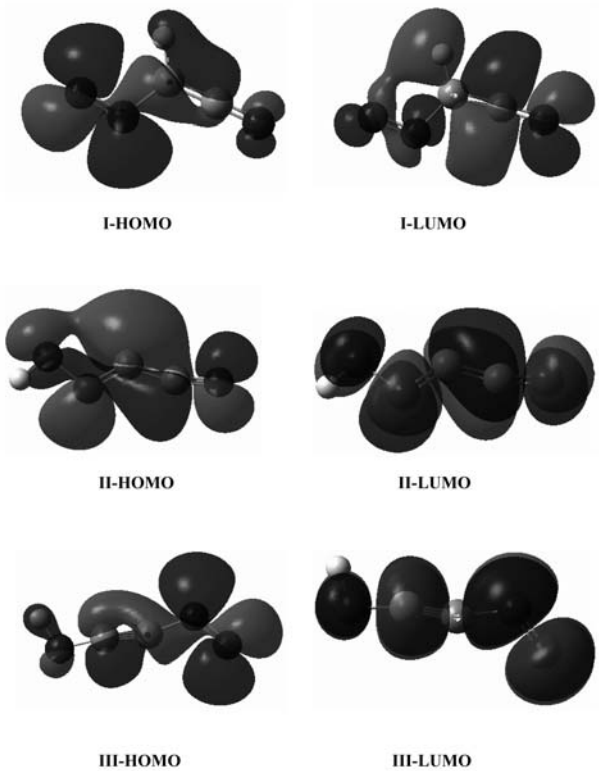

Figure 5. The frontier molecular orbitals (B3LYP/cc-pVDZ), the HOMO and LUMO, of the tautomers concerned. Molecules are oriented according to Figure 2.

Table 6. The HOMO and LUMO energies (ε) of considered species computed at different levels of theory.

	B3LYP/cc–pVDZ			CBS–Q		
	I	**II**	**III**	**I**	**II**	**III**
HOMO	–6.254	–6.557	–6.156	–10.850	–10.361	–11.020
LUMO	–2.333	–2.973	–2.683	1.022	0.592	0.675
Δε	3.921	3.583	3.473	11.872	10.953	11.695

	MP2/6–31++G(d,p)[a]			G3		
	I	**II**	**III**	**I**	**II**	**III**
HOMO	–10.788	–10.049	–11.182	–10.903	–10.538	–11.062
LUMO	1.054	1.090	0.708	1.013	0.392	0.666
Δε	11.842	11.139	11.89	11.915	10.931	11.728

a: Single-point MP2 calculation after RHF/6–31++G(d,p) geometry optimization.
Energies in eV (1 eV = $1.602*10^{-19}$J), $\Delta\varepsilon = \varepsilon_{LUMO}-\varepsilon_{HOMO}$

Table 7. Some calculated geometrical and physicochemical properties of the structures.

	RHF/cc–pVDZ			
	Area	**Volume**	**Refractivity**	**Polarizability**
I	255.19	243.58	15.99	5.19
II	262.92	250.20	14.33	5.19
III	277.75	248.98	16.35	5.19

	RHF/6–31++G(d,p)			
	Area	**Volume**	**Refractivity**	**Polarizability**
I	255.21	244.62	15.99	5.19
II	262.92	250.54	14.33	5.19
III	277.74	248.75	16.35	5.19

Area, volume, refractivity and polarizability values are in the order of 10^{-20} m2, 10^{-30} m3, 10^{-30} m3, 10^{-30} m^3, respectively.

Table 8 shows the computed vibrational frequency and intensity data of concerned molecules in the gas phase at B3LYP/cc-pVDZ level of theory. The lowest vibrational mode in the spectra of I, II and III are calculated to be at 172, 171 and 154 $cm^{-1,}$ respectively with negligible intensities. The band, at 2223.6 cm^{-1}, is similar to that of ketene[15], 2142 $cm^{-1,}$ and acetylketene[15], 2137 cm^{-1} and therefore this peak is assigned as carbonyl stretch of nitrosoketene (the experimental value[15] is 2146 cm^{-1}). Peak at 1322.6 cm^{-1} (experimental value[15] of it as 1314 cm^{-1}) is assigned as the C = C stretch mode of the nitrosoketene. As mentioned in the introduction part, there are some studies concerning the IR spectra of nitrosoketene molecule [15, 20]. However, there is no reported data (either experimental or computed) about them in the literature (to the best of our knowledge). Thus, details of the assignments of tautomers (**II** and **III**) vibrational analysis are not discussed in this study.

Table 8. Calculated vibrational frequencies (cm^{-1}) and IR intensities (km/mol) at B3LYP/cc–pVDZ level for nitrosoketene (**I**) and its tautomers **II** and **III**.

I		**II**		**III**	
I (km/mol)	***ν (cm^{-1})***	***I (km/mol)***	***ν (cm^{-1})***	***I (km/mol)***	***ν (cm^{-1})***
0.00	172.1	0.57	171.7	2.42	154.3
6.44	180.8	8.74	177.3	6.68	169.2
6.11	529.1	13.25	511.4	11.28	290.1
17.61	561.6	0.47	523.9	102.33	404.7
58.40	563.1	71.63	587.1	3.41	476.1
29.40	666.9	36.43	623.0	6.36	579.1
320.52	1017.3	220.38	960.4	75.50	816.7
0.76	1077.4	209.57	1062.5	143.55	1249.9
67.66	1322.6 (1314)[a]	124.49	1415.4	12.24	1324.2
291.78	1579.3	28.14	1714.8	274.75	1543.8
835.65	2223.6 (2146)[a]	961.15	2179.1	441.13	2302.4
10.45	3190.7	126.61	3726.1	138.85	3674.2

[a] Available experimental values[15] are in parenthesis.

4. Conclusions

Within the limitations of the presently performed calculations, nitrosoketene (I) and structure (III) were found to be the most and the least stable tautomers, respectively. Tautomer II, which was found to be the next most stable one after I, might yield accompanying reaction products. Note that the methods presently employed exhibit parallelism in estimating the stability order based on the total energies. However, this is not the case for the frontier molecular orbital energies and controversial results were obtained. According to the deprotonation calculations, all the species should be more acidic than water and the acidity order is III > II > I in the gas phase. Thus, the present study sheds some valuable light on to this reactive molecule and its tautomers by exploring their structural, energetic, electrostatic and vibrational properties.

5. References

1. K. C. Khemani, F. Wudl, *J. Org. Chem*. **1985**, *50,* 3149–3155.
2. T. Li, W. Cheng, J. Liu, X. Xie, H. Cao, *Theochem.* **2006**, *761(1–3),* 83–88.
3. J. S. Kwiatkowski, J. Leszczynski, *Teochem.* **1995**, *342,* 43–49.
4. Sung, T. T. Tidwell, *J. Am. Chem. Soc*. **1998**, *120(13),* 3043–3048.
5. C. Aubry, J. L. Holmes, J. K. Terlouw, *J. Phys. Chem. A* **1997**, *101(33),* 5958–5961.
6. F. Bernardi, A. Bottoni, M. A. Robb, A. Venturuni, *J. Am. Chem. Soc*. **1990**, *112,* 2106–2114.
7. X. Wang, K. N. Houk, *J. Am. Chem. Soc*. **1990**, *112,* 1754–1756.
8. W. D. Allen, H. F. Schaeffer, *J. Chem. Phys.* **1986**, *84,* 2212.
9. R. Leung-Toung, T. T. Tidwell, I. G. Csizmadia, *Theochem.* **1989**,*183,* 319–330.
10. R. Leung-Toung, T. T. Tidwell, *J. Am. Chem. Soc*. **1990**, *112,* 1042–1048.
11. L. A. Burke, *J. Org. Chem.* **1985**, *50,* 3149–3155.
12. M. A. Pericas, F. Serratosa, E. Valenti, *J. Chem. Soc. Perkin Trans. 2*, **1987**, 151–159.
13. M. T. Nguyen, T. Ha, O. R. A. More, *J. Org. Chem.* **1990**, *55,* 3251–3256.
14. L. Gong, M. A. McAllister, T. T Tidwell, *J. Am. Chem. Soc*. **1991**, *113,* 6021–6028.
15. H. Matsui, E. J. Zückerman, N. Katagiri,C. Kaeko, S. Ham, D. M. Birney, *J. Phys. Chem. A* **1997**, *101,* 3936–3941.
16. D. P. Shong, in: S. W. Lander, in: J. M. Leginus, in: C. M. Dicken, in: D. P. Curran (Ed.): Advences in Cycloaddition, JAI Press, Greenwich, **1998**, Vol. 1.
17. P. N. Confalone, E. M. Huie, *Org. React.* **1998**, *36,*1.
18. S. Ham, D. M. Birney, *Tet. Lett.* **1997**, *38(34),* 5925.
19. H. Matsui, N. Kobko, J. J. Dannenberg, S. H. Jonas, R. Visiwanathan, *J. Raman Spect.* **2002**, *33,* 443.
20. H. M. Badawi, W. Förner, *Teochem.* **2001**, *542,* 7–20.
21. J. J. P. Stewart, *J. Comput. Chem*. **1989**, *10,* 209.
22. J. J. P. Stewart, *J. Comput. Chem*. **1989**, *10,* 221.
23. A. R. Leach: Molecullar Modelling, Longman, Essex, **1997**.
24. P. Fletcher: Practical Methods of Optimization, Wiley, New York, **1990**.
25. W. Kohn, *Phys. Rev.* **1965**, *140,* 1133–1138.
26. R. G. Parr, in: W. Yang: Density Functional Theory of Atoms and Molecules, Oxford University Press, London, **1989**.
27. A. D. Becke, *Phys. Rev. A* **1988**, *38,* 3098–3100.
28. S. H. Vosko, L. Vilk, M. Nusair, *Can. J. Phys.* **1980**, *58,* 1200–1211.
29. C. Lee, W. Yang, R. G. Parr, *Phys. Rev. B* **1988**, *37,* 785–789.
30. I. N. Levine: Quantum Chemistry, Prentice Hall, New Jersey, **2000**.
31. L. A. Curtiss, K. Raghavachari, G. W. Trucks, J. A. Pople, *J. Chem. Phys*. **1991**, *94,* 7221–7230.
32. L. A. Curtiss, K. Raghavachari, P. C. Redfern, V. Rassolov, J. A. Pople, *J. Chem. Phys*. **1998**, *109,* 7764–7776.
33. J. A. Montgomery, M. J. Frisch, G. A. Petersson, *J. Chem. Phys*. **1999**, *110,* 2822–2827.
34. N. R. Nyden, G. A. Petersson, *J. Chem. Phys*. **1981**, *75,* 1843–1862.
35. G. A. Petersson, M. A. Al-Laham, *J. Chem. Phys*. **1991**, *94,* 6081–6090.
36. G. A. Petersson, J. A. Trensfeldt, J. A. Montgomery, *J. Chem. Phys*. **1991**, *94,* 6091–6101.
37. J. A. Montgomery, J. W. Oshetrski, G. A. Petersson, *J. Chem. Phys*. **1994**, *101,* 5900–5909.
38. G. A. Petersson, A. Bennett, T. G. Trensfeldt, M. A. Al-Laham, W. A. Shirley, J. Mantzaris, *J. Chem. Phys*. **1988**, *89,* 2193–2218.
39. I. A. Koppel, P. Burk, I. Koppel, I. Leito, T. Sonoda, M. Mishima, *J. Am. Chem. Soc.* **2000,** *122,* 5114–5124.
40. J. W. Oshetrski, G. A. Petersson, K. B. Wilberg, *J. Am. Chem. Soc*. **1995**, *117,* 11299–11308.
41. G. A. Petersson, D. K. Malick, W. G. Wilson, J. W. Oshetrski, J. A. Montgomery, J. A. Frisch, *J. Chem. Phys*. **1999**, *109,* 10570.
42. M. D. Liptak, G. C. Shields, *Int. J. Quantum Chem.* **2001**, *87,* 727.
43. M. J. Frisch, G. W. Trucks, H. B. Schlegel, G. E. Scuseria, M. A. Robb, J. R. Cheeseman, J. A. Jr. Montgomery, T. Vreven, K. N. Kudin, J. C. Burant, J. M. Millam, S. S. Iyengar, J. Tomasi,V. Barone, B. Mennucci, M. Cossi, G. Scalmani, N. Rega, G. A. Petersson, H. Nakatsuji, M. Hada, M. Ehara, K. Toyota, R. Fukuda, J. Hasegawa, M. Ishida, T. Nakajima, Y. Honda, O. Kitao, H. Nakai, M. Klene, X. Li, J. E. Knox, H. P. Hratchian, J. B. Cross, C. Adamo, J. Jaramillo, R. Gomperts, R. E. Stratmann, O. Yazyev, A. J. Austin, R. Cammi, C. Pomelli, J. W. Ochterski, P. Y. Ayala, K. Morokuma, G. A. Voth, P. Salvador, J. J. Dannenberg, V. G. Zakrzewski, S. Dapprich, A. D. Daniels, M. C. Strain, O. Farkas, D. K. Malick, A. D. Rabuck, K. Raghavachari, J. B. Foresman, J. V. Ortiz, Q. Cui, A. G. Baboul, S. Clifford, J. Cioslowski, B. B. Stefanov, G. Liu, A. Liashenko, P. Piskorz, I. Komaromi, R.

L. Martin, D. J. Fox, T. Keith, M. A. Al-Laham, C. Y. Peng, A. Nanayakkara, M. Challacombe, P. M. W. Gill, B. Johnson,W. Chen, M. W. Wong, C. Gonzalez, J. A. Pople, GAUSSIAN 03, Revision B. 03, Gaussian, Inc., Pittsburgh PA, 2003.
44. J. S. Murray, P. Lane, P. Politzer, *Mol. Phys.* **1995***, 85,* 1.
45. P. Politzer, J. S. Murray, *Mol. Phys.* **1996**, *86,* 251–255.
46. P. Politzer, J. S. Murray, *J. Mol. Struct.* **1996**, *376,* 419–424.
47. P. Politzer, P. R. Laurence, L. Abrahmsen, B. A. Zilles, P. Sjoberg, *Chem. Phs. Lett.* **1984**, *111*, 75.
48. J. S. Murray, P. Lane, P. Politzer, *Theochem.* **1990**, *209,* 163–175.
49. P. Politzer, JS. Murray, Energetic Materials, Part2: Detonation, Combustion, Ch. 1, Elsevier, Amsterdam, **2003**.
50. D. M. McQuarrie: Statistical Mechanics, Harper and Row, New York, **1970**.
51. M. D. Liptak, K. C. Gross, P. G. Seybold, S. Feldgus, G. S. Shields, *J. Am. Chem. Soc.* **2002**, *124,* 6421–6427.
52. J. S. Francisko, *J. Chem. Phys.* **2001**, *115(14),* 6373–6375.

Povzetek

Z *ab initio* in DFT računi smo ob uporabi različnih baznih setov raziskovali stabilnost tavtomer nitrozoketena. Z omenjenimi teorijami smo ugotovili, da je najbolj stabilna oblika nitrozoketen (I), najmanj stabilna pa je njegova njegova tavtomera (III). Z uporabo metode Gaussian-2 (G2) smo izračunali deprotonacijsko energijo tavtomer nitrozoketena v plinasti fazi. Na osnovi izračunov deprotonacije lahko ugotovimo, da so vse tavtomerne oblike bolj kisle od vode, po kislosti jih lahko razvrstimo po naslednjem vrstnem redu III > II > I. Vibracijske IR spektre omenjenih molekul v plinski fazi smo izračunali z uporabo gostotnih funkcionalov na osnovi teorije B3LYP in ob uporabi baznega seta cc-pVDZ.